SUPPLEMENTAL FIGURE LEGENDS

Supplementary Figure 1 (linked to Figure 1). Total ephrin-A levels are markedly reduced in motor neurons and mesenchyme of *Efna2*$^{-/-}$;*Efna5*$^{-/-}$ mutants.

(**A, B**) Immunostaining of *Hb9::GFP* transgenic mouse (e11.5) at lumbar level. LMC_L axons (open arrowheads) express ephrin-A5 and EphA4, while LMC_M (arrowhead) axons express only ephrin-A5. Ephrin-A5 and EphA4 are also detected in the ventral (v) and dorsal (d) mesenchyme, respectively. (**C**) *In situ* detection of *EphA7* mRNA in the dorsal limb (open arrowheads point to LMC_L axons).

(**D-F**) Stripe assay with *Hb9::GFP* transgenic lumbar e12.5 mouse explants on alternating EphA7-Fc and ephrin-A5-Fc substrates. EphA4$^+$/GFP$^+$ LMC_L axons prefer the EphA7-Fc substrate. EphA4$^-$/GFP$^+$ LMC_M axons (arrowhead, note large growth cone) do not avoid the ephrin-A5-Fc substrate.

(**G-I'**) Overlay assay with recombinant EphA7-Fc detects the complement of ephrin-As (∑ephrin-A) expressed on dissociated lumbar motor neurons from either control *Efna2*$^{+/-}$; *Efna5*$^{+/-}$;*Hb9::GFP* or *Efna2*$^{-/-}$;*Efna5*$^{-/-}$;*Hb9::GFP* mutant embryos. (**G', I'**) ∑ephrin-A (EphA7-Fc signal) in GFP$^+$ cells is converted to a binary mask that was used for the quantification of ephrin-A puncta in K. (**H, J**) Overlay assay with recombinant EphA3-Fc reveals the cumulative distribution of ephrinAs (∑ephrin-A) on transverse sections of *Efna2*$^{+/-}$;*Efna5* $^{+/-}$ control and *Efna2*$^{-/-}$;*Efna5*$^{-/-}$ mutant e11.5 embryos at the hindlimb level. In controls ephrin-As are detected in the ventral limb, mesenchyme surrounding the spinal cord, DRG, and faintly in the motor columns. EphA3-Fc binding is strongly decreased in double mutants. (**K**) Quantification of ∑ephrin-A in *Efna2*$^{+/-}$; *Efna5* $^{+/-}$ or *Efna2*$^{-/-}$;*Efna5*$^{-/-}$ cells. Mean ± SEM, N cells: *Efna2*$^{+/-}$;*Efna5* $^{+/-}$, 27; *Efna2*$^{-/-}$;*Efna5*$^{-/-}$, 41; (***) $p<0.001$ unpaired t test.

Scale bars: A, B: 100μm; C: 40μm; D-F: 28μm; G-I': 10μm; H, J: 100μm.

Supplementary Figure 2 (linked to Figure 2). Transgenic expression of EphA4^{ECD}-ephrinA5^{GPI} masks endogenous ephrin-As and causes limb innervation defects.

(**A, B**) In control e12.5 mouse embryo sections EphA3-Fc overlay reveals the cumulative distribution of ephrin-As available for binding to EphA receptors (∑ephrin-A^{FREE}) on spinal neurons (SC) and limb tissue. (**C, D**) The EphA4^{ECD}-ephrinA5^{GPI} masking chimera is activated by ubiquitously expressing *EIIa::Cre*. The sites of transgene activation are monitored by expression of RFP driven by a downstream ires signal. Recombinant EphA3-Fc binding to tissue expressing the masking construct is greatly reduced following Cre-activation of the transgene. (**E**) Quantification of EphA3-Fc binding in control and *EphA4^{ECD}-ephrinA5^{GPI};EIIa::Cre* sections. The complement of unoccupied ∑ephrin-A^{FREE} (available for trans-interaction with EphA) is significantly reduced in transgenic embryos. Mean ± SEM, N=15 sections; (***) $p<0.001$ unpaired t test. (**F**) Western blot of *EphA4^{ECD}-ephrinA5^{GPI}* (*Tg*)*;EIIa::Cre* lysates shows robust and specific expression of EphA4^{ECD}-ephrinA5^{GPI} and RFP upon Cre-mediated recombination. ERK is a loading control. (**G, H**) Whole mount neurofilament staining of e12.5 embryos shows the pattern of hindlimb innervation. Greyscale images are inverted to show neurofilament in black. Extension of the peroneal nerve (outlined by red arrowheads) in the dorsal limb is affected by expression of EphA4^{ECD}-ephrinA5^{GPI} activated by the ubiquitous *EIIa::Cre* driver. The nerve appears stunted and defasciculated compared to control embryos (8/10 embryos). (**I-L**) The specificity and timing of *Olig2::Cre*-mediated recombination in motor neurons is confirmed by monitoring ires-RFP expression in *EphA4^{ECD}-ephrinA5^{GPI}(ires-RFP); Olig2::Cre* e11.5 embryos. (**K, L**) RFP and motor neuron-specific VAChT signals precisely overlap in the motor columns and axons that extend into the limb. (**J**) No RFP is detectable in controls. Note that the extension of LMC_L axons is reduced in transgenic embryos (open arrowheads in K, L; compare to I, control) while LMC_M projections are unaffected (arrowheads). (**M, Q**) Lumbar motor axons extend on alternating stripes of control IgG-Fc (grey) and ephrin-A5-Fc (red). Axons (neurofilament) from both control and *EphA4^{ECD}-ephrinA5^{GPI};Olig2::Cre$^{+/-}$* explants avoid

ephrin-A and grow on the permissive IgG-Fc stripes. (**O, P**) The large majority of axons extending from the explants are labeled by the motor neuron marker VAChT. (**Q**) Preference index: ratio between motor axons (neurofilament signal) on IgG-Fc vs. ephrin-A5-Fc stripes. No preferential growth is observed on alternating control IgG-Fc stripes. Controls are wild type or *Olig2::Cre*$^{+/-}$ littermates. Mean ± SEM, N explants: *Control*, 9; *EphA4*^{ECD}*-ephrinA5*^{GPI} (*Tg*)*;Olig2::Cre*$^{+/-}$, 6; (ns) p>0.05; (***) p<0.001 Tukey's test.

Scale bar, A-D: 100μm; G,H: 200μm; I-L: 200μm; M-N: 100μm; O-P: 25μm.

Supplementary Figure 3 (linked to Figure 3). Nerve arborization and guidance phenotypes in GDNF signaling mutants.

(**A-I**) Immunostaining of transverse sections of e11.5 *Hb9::GFP* embryos at hindlimb levels. Ret and p75 receptors are associated with motor axons at the time of dorsoventral projection. (**A-C**) p75 is detected on LMC_L (EphA4$^+$, open arrowheads) and LMC_M axons (solid arrowhead) marked by GFP. (**D-F**) Ret is detected on both LMC_L (EphA4$^+$, open arrowheads) and LMC_M axons (solid arrowhead). (**G-I**) A restricted domain of mesenchymal GDNF expression is visible at the bifurcation point, flanking the LMC_L axons (EphA4$^+$, open arrowheads).

(**J-O**) EphA4 labeling on transverse sections of *Ret*$^{+/-}$ control and *Ret*$^{-/-}$ mutant embryos expressing *Hb9::GFP* to visualize LMC_L axons. (**J, M**) Motor axons reach the base of the limb on schedule (e10.5) in both *Ret*$^{+/-}$ and *Ret*$^{-/-}$ embryos. (**K, L**) In e11.5 *Ret*$^{+/-}$ embryos, EphA4$^+$ LMC_L axons have extended into the dorsal limb mesenchyme (open arrowheads), and EphA4$^-$ LMC_M axons project ventrally (arrowheads). (**N, O**) In e11.5 *Ret*$^{-/-}$ mutant embryos many EphA4$^+$ LMC_L axons inappropriately follow a ventral trajectory, resulting in thinning of the dorsal branch (open arrowheads). Note EphA4 labeling on the ventral axon branch (arrowheads).

(**P**) Dorsal view of the brachial plexus in e12.5 *Ret*$^{+/-}$ embryos expressing *Hb9::GFP* (black, inverted fluorescence) shows the extensive arborization of the medial anterior thoracic (cutaneous, N. cut; orange trace) nerve that innervates the superficial cutaneous maximus (CM)

muscle and the thoracodorsalis nerve (N. th.; purple trace) that innervates the latissumus dorsi (LD) muscle. Other brachial nerves are visible. (**Q**) In *Ret*$^{-/-}$ mutants (N>30 embryos), and (**R**) *Gfra1* $^{-/-}$ mutants (N>25 embryos) the N. cut. and N. th. are absent. The phenotype is fully penetrant in both mutants. (**S**) In *Hb9::Gfra1* transgenic embryos the CM and LD muscles are innervated normally (N>35 embryos).

(**T-AA'**) Dissociated chick motor neurons transfected with GFP-ephrin-A5 and Ret were stimulated with either GDNF (50ng/ml, 15 min) or EphA7-Fc (5mg/ml, 15 min) and subjected to detergent extraction prior to fixation followed by *in situ* Proximity Ligation Assay (PLA) to detect association between Ret/ephrin-A5. In cells left untreated (**T-U'**) or stimulated with EphA7-Fc (**Z-AA'**) Ret is mainly present in membrane-soluble domains and hence sensitive to detergent extraction, whereas GDNF treatment (**V-Y'**) promotes the accumulation of Ret in lipid rafts (See Figure 4U-Z). GFP-ephrin-A5 remains associated with lipid rafts in all conditions. PLA^{+} dots (red) corresponding to sites of Ret/ephrin-A5 interactions are visible on the cell bodies (box in V, W) and distal axons (box in X, Y) in >90% of GFP^{+} GDNF-treated cells. Only sporadic PLA signal is present in untreated or EphA7-Fc-stimulated GFP^{+} cells. The boxed area in T-AA is enlarged in T'-AA'.

(**BB-GG**) SCG neurons were treated with control IgG-Fc or with EphA7-Fc, either alone or in combination with GDNF for 15min or 1hr, and then subjected to Ret51 immunoprecipitation (IP) followed by Western blotting (WB) with the indicated antibodies. (**BB, Top panel**) EphA7-Fc leads to accumulation of tyrosine-phosphorylated Ret (P-Ret51). GDNF induces Ret phosphorylation, which is further augmented by EphA7-Fc co-stimulation. (**BB, Middle panel and CC**) Ret levels augment upon stimulation with EphA7-Fc. GDNF induces an increase in Ret levels at 15min followed by clearance of the receptor at 1 hr, which is attenuated by EphA7-Fc co-stimulation. The ratio between phosphorylated and total Ret is reported below each lane. Quantification of total Ret levels from > 4 experiments is shown in CC. (**DD, GG**) EphA7-Fc potentiates GDNF signaling. Supernatants from the IP shown in BB were analyzed by WB with

antibodies against phopho-ERK (**DD**) and phospho-Akt (**FF**). EphA7-Fc alone does not induce significant ERK or Akt phosphorylation but enhances the effects of GDNF. (**EE**, **GG**) Quantification of phospho-ERK1 (**EE**) and phospho-Akt (**GG**) levels from > 4 experiments; (*) $p<0.05$ unpaired t test. Actin (bottom panels in BB, DD, FF) serves as a loading standard.

Scale bar: A-F: 200μm; G-I: 100μm; J-O: 100μm; P-S: 200μm; T-AA: 10μm; T'-AA': 3μm.

Supplementary Figure 4 (linked to Figure 4). In vitro studies of ephrin-A reverse and forward signaling.

(**A-H**) Ephrin-A reverse signaling promotes motor axon outgrowth. (**A-D**) Minimal motor axon growth from *Hb9::GFP*$^{+}$ lumbar LMC explants cultured for ~20h is observed on control IgG-Fc substrates. (**E-H**) Robust GFP^{+} motor axon growth occurs on EphA7-Fc used to activate ephrin-A reverse signaling. (**D, H**) β3-tubulin signal associated with GFP^{-} non-motor neurons (non-MN) reveals that motor neurons are more responsive to EphA7-Fc than other neuronal populations present in the explants. The growth response of 'non-MN' axons is quantified in Figure 4S.

(**I-P**) EphA-mediated axon repulsion does not require GDNF:Ret signaling. (**I-K**) Lumbar motor axons extend on alternating stripes of control IgG-Fc (grey) and ephrin-A5-Fc (red). Both *Ret*$^{+/-}$ and *Ret*$^{-/-}$ motor axons (*Hb9::GFP*$^{+}$) exhibit a strong avoidance response to ephrin-A and grow on the permissive IgG-Fc stripes. (**K**) Preference index: ratio between motor axons (GFP signal) on IgG-Fc vs. ephrin-A5-Fc stripes. No preferential growth is observed on alternating control IgG-Fc stripes. Mean ± SEM, N explants: *Ret*$^{+/-}$, 5; *Ret*$^{-/-}$, 4; (ns) $p>0.05$; (***) $p<0.001$ Tukey's test.

(**L-P**) Lumbar motor explants from *Ret*$^{+/-}$, *Ret*$^{-/-}$, or *EphA4*$^{-/-}$ embryos with the *Hb9::GFP* reporter stimulated with control IgG-Fc or increasing doses of clustered ephrin-A1-Fc for 1h to activate EphA- forward signaling that leads to growth cone collapse (compare **L** and **M**, arrowheads). (**M, N**) Growth cone collapse is similar in control *Ret*$^{+/-}$ and *Ret*$^{-/-}$ mutants (arrowheads), but is severely impaired in *EphA4*$^{-/-}$ mutants, reflecting the sensitivity of the assay (arrowheads in **O**).

(**P**) Growth cone collapse dose-response curve for indicated mutants. The concomitant application of ephrin-A1-Fc and GDNF (100ng/ml, 1h) does not affect growth cone collapse in either *Ret*$^{+/-}$ or *Ret*$^{-/-}$ axons. *EphA4*$^{+/-}$ axons show decreased growth collapse at intermediate concentration of ephrin-A1-Fc. Mean ± SEM, >150 growth cones per condition; (**) $p<0.01$; (***) $p<0.001$ Dunnett's test vs control *Ret*$^{+/-}$ at the corresponding ephrin-A1-Fc dose; other conditions were not significantly different from control ($p>0.05$).

Scale bar, A-H: 200μm; I-J: 100μm; L-O: 13μm

Supplementary Figure 5 (linked to Figure 5). Expression of Ret and GFRα1 in lumbar motor neurons.

(**A-D'**) *In situ* detection of *Ret* and *Gfra1* mRNA in the lumbar LMC (outlined) in serial transverse sections at e11.5 and e12.5 mouse embryos. Isl1 staining, either on the same (A', C', D') or adjacent (B') sections, marks the medial division of the LMC. mRNA signal is pseudocolored in green and overlaid with Isl1 staining (red) in A', B', C', D'. At both e11.5 and 12.5, *Ret* is enriched in LMC_L neurons ($Isl1^-$), while *Gfra1* is highest in LMC_M neurons (overlaps with Isl1).

(**E-H**) Anti-FLAG staining (red) detects FLAG-tagged GFRα1 in *Hb9::GFP*$^+$ motor neuron cell bodies (arrowhead) and axons (open arrowhead) driven by the *Hb9::Gfra1* transgene in e10.0 embryos. No FLAG signal (red) is visible in wild type embryos.

Scale bar, A-E': 120μm; F-I: 100μm.

Supplementary Figure 6 (linked to Figure 6). GDNF chemoattraction is normal in *Hb9::Gfra1* motor neuron explants.

(**A**) Attraction assay: lumbar motor explants cultured for ~15h in 3D collagen/matrigel matrices next to agarose beads soaked with growth factors (GDNF, HGF) or BSA on the proximal side (P),

and control beads soaked with BSA on the distal (D) side. The P and D sides of the explant correspond to the two halves of the ventral spinal cord, containing the left and right motor columns and the floor plate in between. Expression of *Hb9::GFP* allows visualization of motor axons extending from the explants.

(**B**) Directional growth: quantification of the ratio (P:D) between axon growth (GFP pixels) on the P vs. D sides (mean ± SEM). (**C**) Since the GDNF gradient has a (weaker) outgrowth effect on the D side, which decreases the P:D ratio, quantification of motor axon growth from the P side is also reported. Mean ± SEM, N explants: *WT*, BSA (13), *WT*, HGF (14), *WT*, GDNF (27), $Ret^{-/-}$, GDNF (16), *Hb9::Gfra1*, GDNF (7); (ns) $p>0.05$; (***) $p<0.001$ Dunnett's test vs *WT*/BSA; (NS) $p>0.05$ unpaired t test *WT*/GDNF vs *Hb9::Gfra1*/GDNF.

(**D**) No motor axon growth is observed in the presence of BSA-beads on the either side. (**E**) GDNF-beads stimulate robust, directional, motor axon growth from the P side. (**F**) GDNF-triggered attraction is abolished in $Ret^{-/-}$ mutants. (**G**) The attraction response of *Hb9::Gfra1* transgenic explants to GDNF is comparable to controls. HGF-induced chemoattraction is used as a positive control.

Scale bar, 100μm

SUPPLEMENTAL EXPERIMENTAL PROCEDURES

Mouse lines

EphA4^{ECD}-ephrinA5^{GPI} transgenic mice: Although the ideal approach for examining the role of ephrin-A reverse signaling in axon guidance is to analyze *ephrin-A* mouse mutants, the expression of ephrin-As on both axons and mesenchymal cells does not permit the discrimination of ligand and receptor functions using conventional null mutants. To dissociate the receptor and ligand functions of ephrin-As we considered tissue specific knockouts but this proved difficult because of the redundancy of ephrin-A expression in motor neurons and limb tissues. In light of these issues we devised a strategy to mask all ephrin-A reverse signaling in motor neurons by initiating futile protein interactions with the chimeric protein EphA4^{ECD}-ephrinA5^{GPI}.

Cloning of the EphA4^{ECD}-ephrinA5^{GPI} chimera has been previously described (Marquardt et al., 2005). A FLAG-tag is added at the 5' of EphA4^{ECD} following the signal sequence. The EphA4^{ECD}-ephrinA5^{GPI} cDNA was inserted in a modified pCAGEN plasmid, under the CAGGS promoter, and preceded by a 3x poly-A STOP cassette flanked by LoxP sites. EphA4^{ECD}-ephrinA5^{GPI} cDNA is followed by an IRES signal driving expression of monomeric membrane-associated Cherry fluorescent protein.

Hb9::Gfra1 transgenic mice: A FLAG-tag was inserted between the signal sequence and the start codon of mouse *Gfra1* cDNA. The fusion construct was inserted at the 3' end of a 9.2Kb promoter region of the mouse *Hb9* gene (Arber et al., 1999; Thaler et al., 1999). The construct utilizes an SV40 poly-A sequence.

DNA constructs

Plasmids containing mouse *ephrin-A5* and *ephrin-A2* cDNA fused to either V5- or HA-tags in *pCAGGS-ires-gfp* or *pcDNA3.1* (Lim et al., 2008; Marquardt et al., 2005) and the DCC-HA expression plasmid (Stein and Tessier-Lavigne, 2001) were previously described.

EGFP cDNA in the *pEGFP-N1* (Clontech) vector was replaced with HA-tag, to generate *pN1-HA*. For Ret-HA, Slitrk1-HA, p75-HA, the coding sequence of mouse *Ret9*, human *Slitrk1*, or rat *p75* were PCR-amplified from cDNA clones and inserted into *pN1-HA* in frame with the 5' of HA. For Ret-mCherry, the HA tag in Ret-HA was replaced with *mCherry* cDNA. For FLAG-Ret, *Ret9* cDNA was inserted at the 3' of FLAG-tag in the *pCAGGS-FLAG-ires-gfp* expression vector (Marquardt et al., 2005). The FLAG-tag is inserted between the signal sequence and the first codon of *Ret9*. For HA-GFRα1 and FLAG-GFRα1, mouse *Gfra1* cDNA was inserted at the 3' of HA-tag or FLAG-tag in the *pCAGGS-HA-ires-gfp* or *pCAGGS-FLAG-ires-gfp* expression vectors, respectively (Marquardt et al., 2005). For GFP-ephrin-A5, *ephrin-A5* was inserted at the 3' of *EGFP* in *pEGFP-N1*. cDNA clones of mouse *Ret9* (BC059012*)*, mouse *Gfra1* (BC054378), human *Slitrk1* (BC051738) were from Open Biosystems; rat *p75* cDNA was a kind gift of Kuo-Fen Lee (Salk Institute).

Explant and dissociated cell cultures

Motor neuron explants and dissociated cultures were maintained in motor neuron (MN) media': Neurobasal media containing B27 supplement, 2mM L-Glutamine, 25μM L-Glutamate, and 1% Penicillin/Streptomycin (all reagents were from Gibco/Invitrogen). The motor columns were dissected from e12.5 mouse embryos or E3.5-4 chick embryos and dissociated with trypsin essentially as described in Kaeck and Banker (2006). After dissociation, cells were plated on coverslips coated with PDL (100μg/ml)/laminin (1.5-5μg/ml) in MN media supplemented with 10% horse serum for 1-2 hrs, then replaced with regular MN media, and cultured for ~15 hrs unless otherwise indicated.

For growth cone collapse or neurite outgrowth/attraction assays, recombinant chimeric Ephrin-A-Fc and EphA-Fc proteins, respectively, were clustered with 1:5 (mass concentration ratio) anti-

human IgG-Fc antibody (Jackson ImmunoResearch) in PBS or MN media for 1 hr (RT) on a nutator. Clustered human IgG-Fc fragment (Jackson ImmunoResearch) was used as a control.

For growth cone collapse assay, explants were cultured on PDL/laminin^{high} (50μg/ml) for ~20 hrs and stimulated with clustered ephrin-A1-Fc (R&D Systems) at the indicated concentrations for 1 hr at 37°C before fixation and staining.

For bead-attraction assay, the entire caudal half of the lumbar motor columns (including the in-between floor plate) was embedded (ventral side down) in rat tail collagen (50 μl):Matrigel (30 μl) mix (BD Biosciences) for ~15 hrs in MN media in the presence of agarose beads (Sigma) soaked with GDNF (1μg/ml), HGF (10μg/ml), or BSA. The beads were incubated for 3-5 hrs at 4°C in PBS containing the indicated factors, and washed 3-4 times with PBS before use.

SGC primary cultures form Sprague-Dawley rat embryos (Charles River Laboratories) were prepared as previously described (Pierchala et al., 2007) and maintained in DMEM supplemented with 10% FBS, glutamine, 1% Penicillin/Streptomycin and 50 ng/ml NGF (Harlan Biosciences).

Cos-7 and AD293 cells were cultured in DMEM supplemented with 10% FBS, 1% L-Glutamine, 1% Penicillin/Streptomycin.

Dunn chamber assay

Dunn chamber guidance assays were performed as described (Yam et al., 2009). Lumbar LMC neurons were dissociated with trypsin and seeded on nitric acid-treated #3 square coverslips coated with PDL/laminin (5μg/ml). Cells were growth in MN media for ~5 hrs before the chamber was assembled. GDNF (200ng/ml), clustered EphA7-Fc (5μg/ml) or IgG-Fc (5μg/ml) were added to the outer well of the chamber.

Immunostaining, Affinity probes and *in situ* Hybridization

For cryosectioning, embryos were fixed in 4% paraformaldehyde (PFA) diluted in 0.1M phosphate buffer for 2-3 hrs (4°C), washed extensively in PBS, cryoprotected in 30% sucrose ON at 4°C, and embedded in OTC compound. Cryosections (30-60μm) were incubated with primary (ON, 4°C) or secondary antibodies (2-3 hrs, RT) in PBS containing 1% BSA (Jackson ImmunoResearch) and 0.2-0.5% Tx-100 (higher concentration of detergent was used for thicker tissue sections). Sections were mounted with Vectashield (Vector Labs) or PermaFluor (Thermo Scientific). Whole mount immunohistochemistry of e12.5 embryos was performed with anti-neurofilament 2H3 supernatant (Developmental Hybridoma Bank, 1:50) as described (Kitsukawa et al., 1997). For visualization of *Hb9::GFP* fluorescence in whole mount preparations, embryos were eviscerated, fixed, cleared by consecutive 2-4 hr-incubations (4°C) in glycerol 30%, 50%, 80% and mounted between two glass coverslips.

Explants were fixed in 0.1M phosphate buffer containing 4% PFA and 4% sucrose for 30 min at RT, washed in PBS, and incubated with primary and secondary antibodies for 1-2 hrs at RT in the presence of 0.2% Tx-100.

Surface staining of dissociated motor neurons was performed after 15 min fixation followed by blocking with 1%BSA/2%Horse Serum (in PBS) for 30 min at RT. Incubation with primary and secondary antibodies was carried out for 30-40 min (RT) in blocking buffer.

Detergent extraction of dissociated motor neurons was performed essentially as described in Ledesma et al. (1998). Chick motor neurons expressing Ret-Cherry and either V5-ephrin-A5 or GFP-ephrin-A5 were stimulated with GDNF (50ng/ml) or clustered EphA7-Fc (5μg/ml) for 15 min, incubated in 1% Triton X-100 on ice for 5 min prior to fixation (15 min) and staining.

For the PLA (Duolink, Olink Bioscience) experiments shown in Figure 3, chick motor neurons expressing either Ret-Cherry or DCC-HA were incubated for 30min at RT with unclustered recombinant EphA7-Fc (R&D Systems, 5μg/ml) to detect endogenous ephrin-As prior to fixation (15min) and surface staining with either goat anti-Ret or mouse anti-DCC antibodies followed by

PLA probes according to the manufacturer's instructions. The anti-human PLA probe to detect the human IgG1-Fc portion of recombinant EphA7-Fc was generated using Duolink II Probemaker (Olink Bioscience). Cells were marked by GFP expression from co-transfected *pCAGGS-ires-gfp* plasmid. For the PLA experiments shown in Figure S3, chick motor neurons expressing Ret-Cherry and GFP-ephrin-A5 were stained after detergent extraction with anti-Ret and anti-GFP antibodies followed by PLA probes. Commercial and custom-made anti-Ret antibodies could not be used to detect endogenous Ret due to non-specific labeling. However, mouse-specific anti-Ret antibodies were suitable for immunodetection of transfected mouse-Ret in chick motor neurons.

Primary antibodies used for immunostaining were as follows: mouse anti-DCC (Abcam, extracellular epitope 1:500), goat anti-ephrin-A5 (R&D systems 1:100), rabbit anti-EphA4 (Santa Cruz Biotechnology, intracellular epitope, 1:500), mouse anti-FLAG (Sigma 1:1000), guinea pig anti-FoxP1 [(Dasen et al., 2008) 1:10,000], goat anti-GDNF (R&D Systems 1:200), goat anti-GFRα1 (R&D Systems 1:300), rabbit and mouse anti-GFP (Invitrogen 1:2000), rabbit anti-Isl1 (#6594 1:8000), rabbit anti-Isl1/2 [(Ericson et al., 1992) 1:2,500], mouse anti-Neurofilament (2H3, Developmental Studies Hybridoma Bank 1:50 for whole embryo staining; 1:250 for staining of explants), goat anti-p75 (R&D Systems 1:500), goat anti-Ret (R&D Systems, extracellular epitope, 1:100), goat anti-Ret (Neuromics, extracellular epitope, 1:300), rabbit anti-RFP (MBL International 1:3000 for immunohistochemistry; 1:250 for immunocytochemistry), mouse anti-β3 tubulin (Novus Biologicals 1:2000), rabbit anti-VAChT (Synaptic Systems 1:5000), goat anti-VAChT (Millipore 1:5000), mouse anti-V5 (Invitrogen 1:500).

Secondary antibodies were: donkey anti-rabbit/mouse/goat/guinea pig Alexa Fluor 488-, 555-, 647-conjugated (Molecular Probes/Invitrogen 1:750); Cy3-, Cy5-conjugated anti-human IgG, Fcγ antibody (Jackson IR 1:500); Alexa Fluor 555-Phalloidin (Molecular Probes/Invitrogen 1:200) was applied together with secondary antibodies.

Affinity probe detection of ephrin-A on tissue sections using recombinant EphA3-Fc (R&D Systems, 5μg/ml) was performed as previously described (Marquardt et al., 2005). For ephrin-A detection on dissociated motor neurons, recombinant EphA7-Fc (R&D Systems, 5μg/ml) was applied to cells for 30 min at RT prior to fixation (15 min) and staining with Cy3-conjugated anti-human IgG-Fc antibody (Jackson ImmunoResearch). Affinity probe detection of EphA on tissue sections using AP-ephrin-A5-Fc (Feldheim et al., 1998) was performed as described (Giger et al., 1998).

In situ hybridization was performed as described in Birren et al. (1993) with some modifications. *In situ* probes: *EphA7* (kind gift of Greg Lemke, Salk Institute), Ret (X67812; 1245-1891bp), *Gfra1* (BC054378; 1061-1988bp).

Retrograde Fills

Embryos were eviscerated and incubated in DMEM/F-12 (Gibco/Invitrogen) aerated with 95% O2/5% CO2 on a heating plate adjusted to keep the media at ~30°C. Fluorescent dextran (3000 MW lysine fixable rhodamine-cojugated; Molecular Probes/Invitrogen) was pressure injected with a pulled glass needle in either the limb mesenchyme or, in embryos expressing *Hb9::GFP*, directly in the stump of the nerve severed with microscissors. Media was partially replaced every ~30 min. After 6 hrs the embryos were fixed and processed for immunohistochemistry.

In ovo electroporation

Chick eggs (Charles River and McIntyre Farms) were incubated in a humidified chamber, and embryos were staged according to HH (Hamburger and Hamilton, 1992). DNA constructs were injected into the lumens of HH stage 18-19 chick embryonic spinal cords. Electroporation was performed using a square wave electroporator (BTX). Chick embryos were harvested and analyzed after 24-48 hrs.

Immunoprecipitation and Western blotting

AD293 cells were transfected with FugeneHD (Roche Applied Science) for ~20 hrs and lysed for 1 hr at 4°C in lysis buffer (10mM Tris-HCl pH7.4, 137mM NaCl, 2mM EDTA, 10% glycerol) containing 0.5% Triton X-100 and 1% β-octylglucoside (Pierce/Thermo Scientific) (Paratcha et al., 2003) and supplemented with protease (Roche Applied Science) and phosphatase (Halt, Pierce/Thermo Scientific) inhibitor cocktails. Protein lysates were clarified by centrifugation at 13,000 xg for 15 min. 200-400µg of total protein lysate diluted to 500µl with 0.5% Tx-100 lysis buffer were immunoprecipitated with 1-2µg of the indicated antibody ON (4°C), followed by incubation with 50µl of 50% protein A/G bead slurry (Santa Cruz Biotechnology) for 2 hrs (4°C). The beads were washed 4 times with 0.5% Tx-100 lysis buffer and resuspended in NuPAGE LDS sample buffer (Invitrogen). Precipitates were subjected to western blotting with NuPAGE 4-12% Bis-Tris gels (Invitrogen) and probed with the indicated antibodies. Western blot for total cell lysates (Inputs) was performed with 10-20µg of total protein per sample.

Detergent-resistant membranes were prepared from MCF-7 cells expressing V5-ephrin-A5 as described in Paratcha et al. (2001) with minor modifications. After starvation ON and stimulation with either GDNF or EphA7-Fc, cells monolayers were lysed for 1 hr at 4°C in buffer containing 1% Triton X-100, followed by centrifugation at 20,000 xg for 15 min to separate detergent-soluble (supernatant) and detergent-insoluble (pellet) fractions. The pellet was solubilized in the above lysis buffer containing 0.2% SDS for 1 hr at 4°C, sonicated for 5 sec, centrifuged and resuspended in NuPAGE LDS sample buffer.

Mouse spinal cords were lysed and subjected to western blot analysis as previously described (Bai et al., 2011).

SCG neurons were deprived of NGF ON and stimulated as indicated with GDNF (10ng/ml), clustered EphA7-Fc (10µg/ml), or clustered IgG-Fc (10µg/m). After stimulation, cells were

gently washed twice with PBS, and lysed with immunoprecipitation buffer as previously described (Pierchala et al., 2007). Ret51 was immunoprecipitated using Ret51-selective antibodies (C20; Santa Cruz Biotechnology). The precipitates and supernatants were subjected to SDS-PAGE and immunoblotting with antibodies against Ret51, phospho-tyrosine, phospho-AKT, phospho-ERK1/2 (all reagents from Cell Signaling), or actin (I19, Santa Cruz Biotechnology) as indicated. Other antibodies used for immunoblotting include: rabbit anti-RFP (MBL International), mouse anti-FLAG (Sigma), mouse anti-HA (Covance), HRP-conjugated mouse anti-HA (Sigma), anti-V5 (Invitrogen).

Image analysis and Quantification

Whenever possible, images used for quantification were acquired using the same microscope settings and adjusted to the same background levels.

For quantification of the stripe assay, *Hb9::GFP* fluorescence of axons growing on either the first or the second set of stripes was measured with Photoshop (Adobe Systems) using the 'select color range' command.

For quantification of EphA7-Fc binding to dissociated neurons, the total number of pixels of anti-human Fc signal was measured with NIH ImageJ using the 'analyze particle' command on thresholded images.

For quantification of nerve growth in $EphA4^{ECD}$-$ephrinA5^{GPI}$ transgenic embryos, serial transverse sections encompassing the entire sciatic plexus were acquired for each embryo and the total number of pixels of VAChT signal (i.e., motor axons) was measured for either the dorsal or ventral nerve branch using Photoshop. EphA4 signal intensity (# pixels x mean fluorescence) associated with either nerve branch was also measured for each section.

The size of the peroneal nerve was quantified in whole mount embryo preparations by manually outlining the nerve, visualized through *Hb9::GFP* fluorescence, and measuring GFP signal intensity. To account for embryo-to-embryo variability in *Hb9::GFP* levels, the fluorescence of a

characteristic ectopic site of *Hb9::GFP* expression was used to normalize nerve-associated fluorescence in each embryo.

A semi-automated quantification of axon outgrowth from motor explants was performed using the FeatureJ plugin of NIH ImageJ (Grider et al., 2006) that uses a Hessian-based algorithm to detect linear structures, such as axons. The algorithm was applied to images of *Hb9::GFP* fluorescent axons after removal of the signal associated with the motor columns to measure the total axonal area (#pixels).

The percentage of growth cone collapse was quantified as previously described (Gallarda et al., 2008).

Pearson's correlation coefficients were calculated using the Coloc_2 plugin of NIH ImageJ/Fiji.

Quantification of immunoblots was performed with NIH ImageJ.

The unpaired t test (two-tailed), Dunnett's multiple comparison test (after one-way ANOVA) and Tukey's multiple comparison test (after one-way ANOVA) were performed with GraphPad Prism software. The Kolmogorov-Smirnov test was performed with IGOR Pro software. $p<0.05$ was considered significant.

Microscopes

Fluorescence-assisted microdissections were performed with a Zeiss Lumar V12 microscope. The same instrument was used for imaging of whole mount neurofilament staining. Representative images of the peroneal nerve of *Hb9::Gfra1* and control embryos were acquired with a Praire Technologies Ultima two-photon microscope. Images were acquired with 4x (for whole mount preparations), 10x, 20x, 60x objectives on an Olympus Fluoview 1000 confocal microscope. For the Dunn's chamber assay, a long distance 20x objective was used. With the exception of surface staining and PLA detection on growth cones, which were acquired as single confocal sections, all other images correspond to maximal Z-projections of confocal stacks. To obtain the whole motor

projection pattern at the sciatic plexus, confocal stacks acquired from adjacent transverse sections were combined using the Mosaic plugin of NIH ImageJ.

SUPPLEMENTAL REFERENCES

Arber, S., Han, B., Mendelsohn, M., Smith, M., Jessell, T.M., and Sockanathan, S. (1999). Requirement for the homeobox gene Hb9 in the consolidation of motor neuron identity. Neuron *23*, 659-674.

Birren, S.J., Lo, L., and Anderson, D.J. (1993). Sympathetic neuroblasts undergo a developmental switch in trophic dependence. Development *119*, 597-610.

Dasen, J.S., De Camilli, A., Wang, B., Tucker, P.W., and Jessell, T.M. (2008). Hox repertoires for motor neuron diversity and connectivity gated by a single accessory factor, FoxP1. Cell *134*, 304-316.

Dessaud, E., Yang, L.L., Hill, K., Cox, B., Ulloa, F., Ribeiro, A., Mynett, A., Novitch, B.G., and Briscoe, J. (2007). Interpretation of the sonic hedgehog morphogen gradient by a temporal adaptation mechanism. Nature *450*, 717-720.

Ericson, J., Thor, S., Edlund, T., Jessell, T.M., and Yamada, T. (1992). Early stages of motor neuron differentiation revealed by expression of homeobox gene Islet-1. Science *256*, 1555-1560.

Feldheim, D.A., Vanderhaeghen, P., Hansen, M.J., Frisen, J., Lu, Q., Barbacid, M., and Flanagan, J.G. (1998). Topographic guidance labels in a sensory projection to the forebrain. Neuron *21*, 1303-1313.

Giger, R.J., Urquhart, E.R., Gillespie, S.K., Levengood, D.V., Ginty, D.D., and Kolodkin, A.L. (1998). Neuropilin-2 is a receptor for semaphorin IV: insight into the structural basis of receptor function and specificity. Neuron *21*, 1079-1092.

Grider, M.H., Chen, Q., and Shine, H.D. (2006). Semi-automated quantification of axonal densities in labeled CNS tissue. J Neurosci Methods *155*, 172-179.

Hamburger, V., and Hamilton, H.L. (1992). A series of normal stages in the development of the chick embryo. 1951. Dev Dyn *195*, 231-272.

Kaech, S., and Banker, G. (2006). Culturing hippocampal neurons. Nat Protoc *1*, 2406-2415.

Kitsukawa, T., Shimizu, M., Sanbo, M., Hirata, T., Taniguchi, M., Bekku, Y., Yagi, T., and Fujisawa, H. (1997). Neuropilin-semaphorin III/D-mediated chemorepulsive signals play a crucial role in peripheral nerve projection in mice. Neuron *19*, 995-1005.

Ledesma, M.D., Simons, K., and Dotti, C.G. (1998). Neuronal polarity: essential role of protein-lipid complexes in axonal sorting. Proc Natl Acad Sci U S A *95*, 3966-3971.

Lee, S.K., Jurata, L.W., Funahashi, J., Ruiz, E.C., and Pfaff, S.L. (2004). Analysis of embryonic motoneuron gene regulation: derepression of general activators function in concert with enhancer factors. Development *131*, 3295-3306.

Paratcha, G., Ledda, F., Baars, L., Coulpier, M., Besset, V., Anders, J., Scott, R., and Ibanez, C.F. (2001). Released GFRalpha1 potentiates downstream signaling, neuronal survival, and differentiation via a novel mechanism of recruitment of c-Ret to lipid rafts. Neuron *29*, 171-184.

Pierchala, B.A., Tsui, C.C., Milbrandt, J., and Johnson, E.M. (2007). NGF augments the autophosphorylation of Ret via inhibition of ubiquitin-dependent degradation. J Neurochem *100*, 1169-1176.

Stein, E., and Tessier-Lavigne, M. (2001). Hierarchical organization of guidance receptors: silencing of netrin attraction by slit through a Robo/DCC receptor complex. Science *291*, 1928-1938.

Thaler, J., Harrison, K., Sharma, K., Lettieri, K., Kehrl, J., and Pfaff, S.L. (1999). Active suppression of interneuron programs within developing motor neurons revealed by analysis of homeodomain factor HB9. Neuron *23*, 675-687.

Yam, P.T., Langlois, S.D., Morin, S., and Charron, F. (2009). Sonic hedgehog guides axons through a noncanonical, Src-family-kinase-dependent signaling pathway. Neuron *62*, 349-362.

Supplemental Figure 1

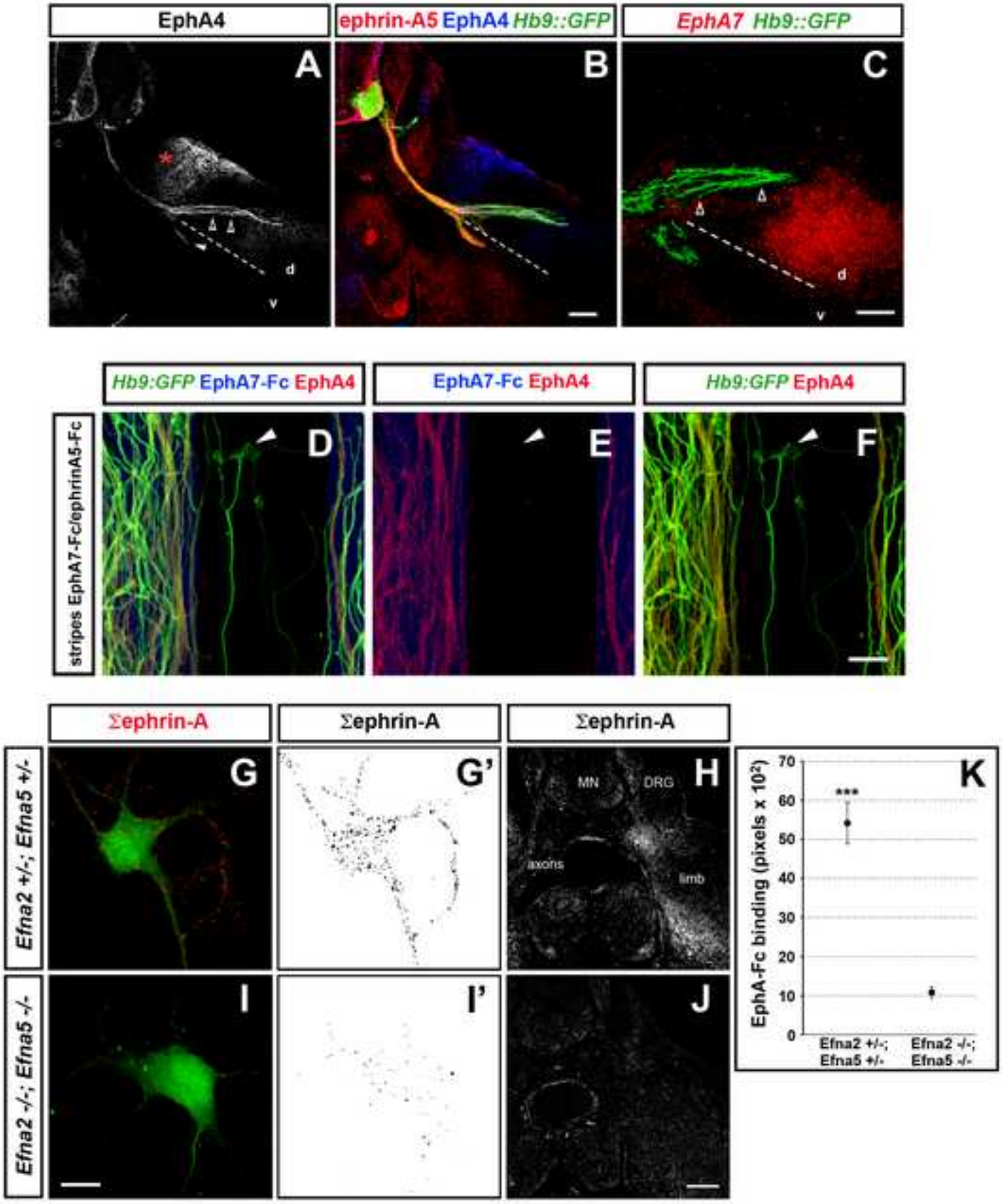

Supplemental Figure 2

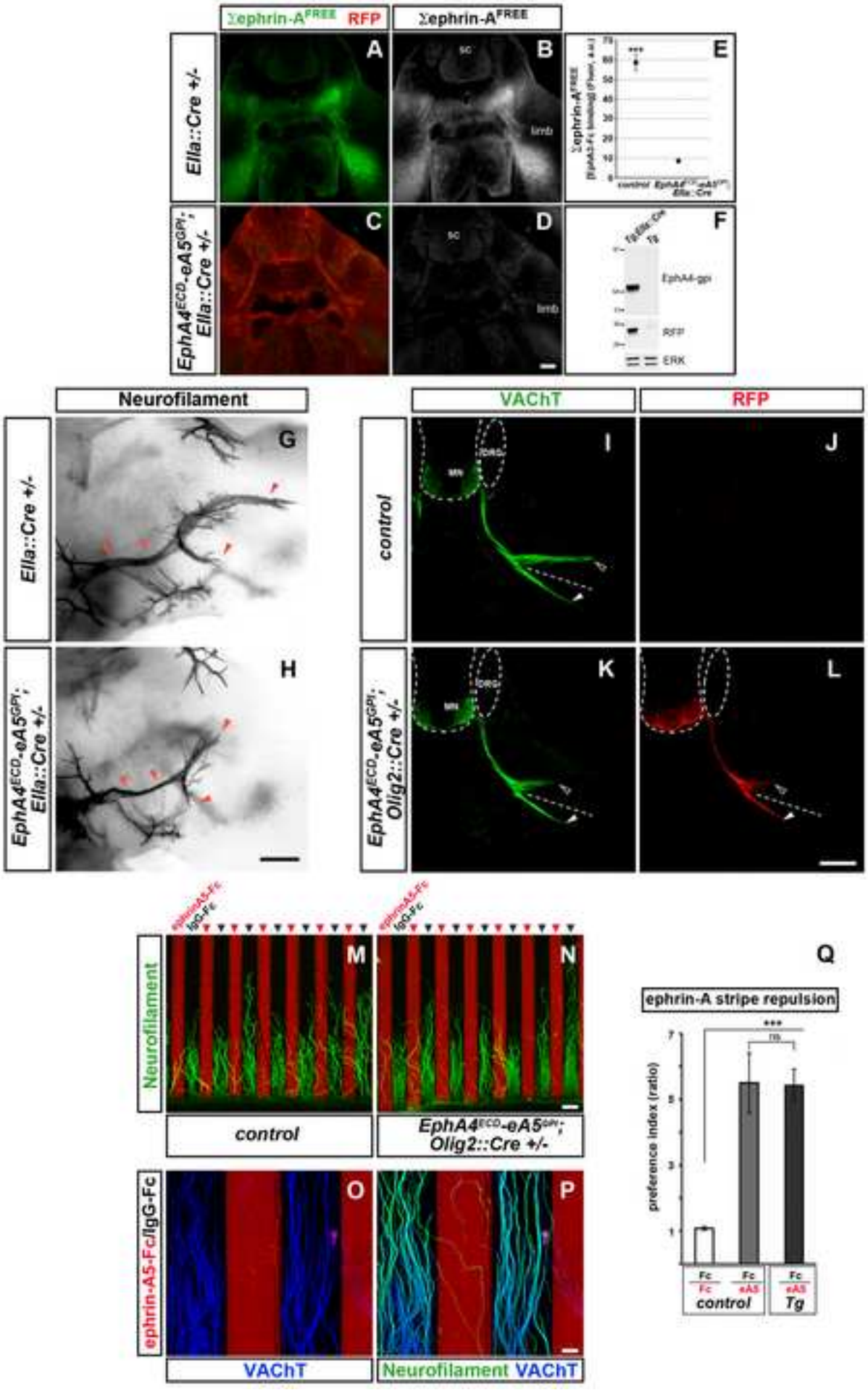

Supplemental Figure 3

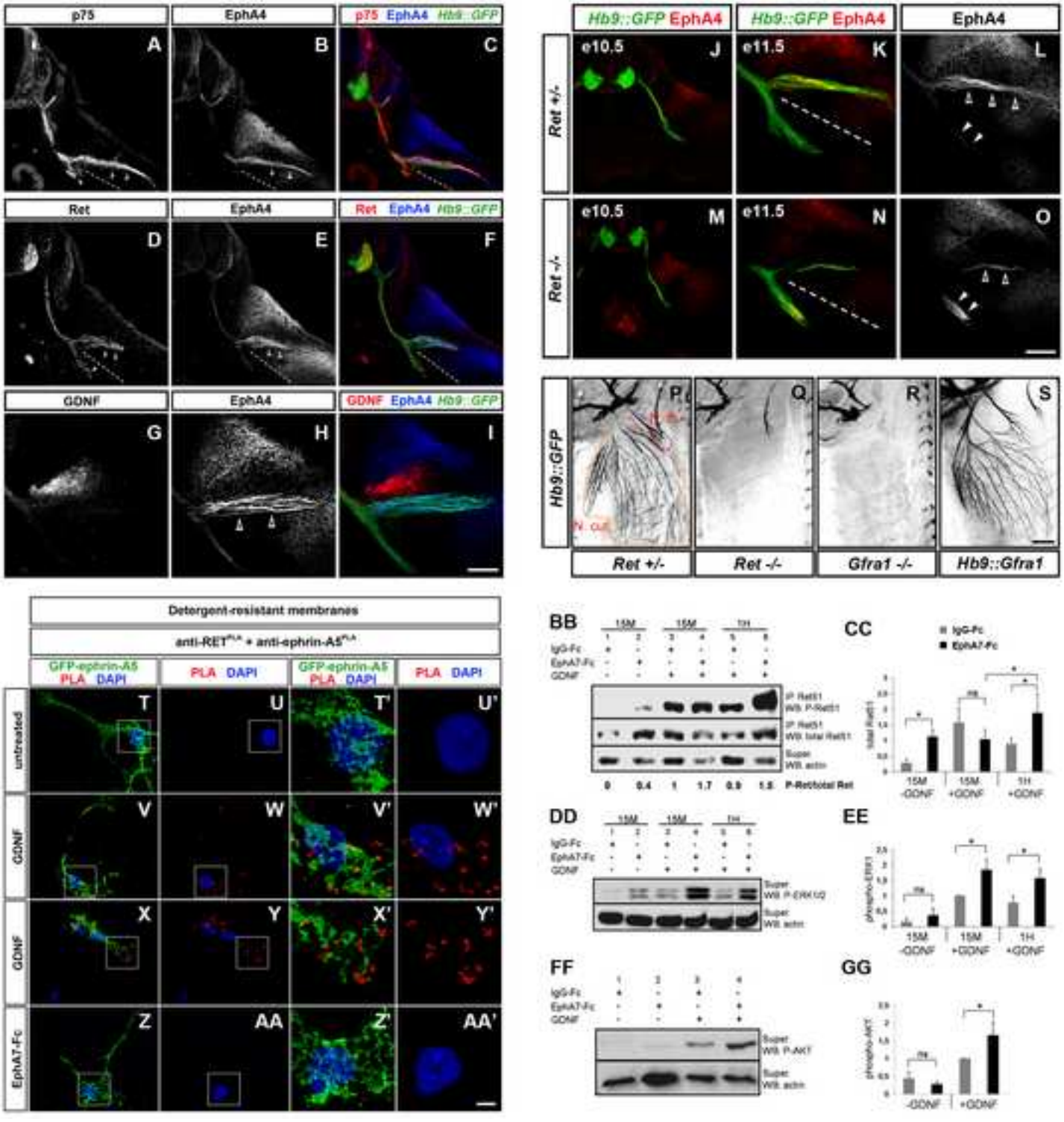

Supplemental Figure 4

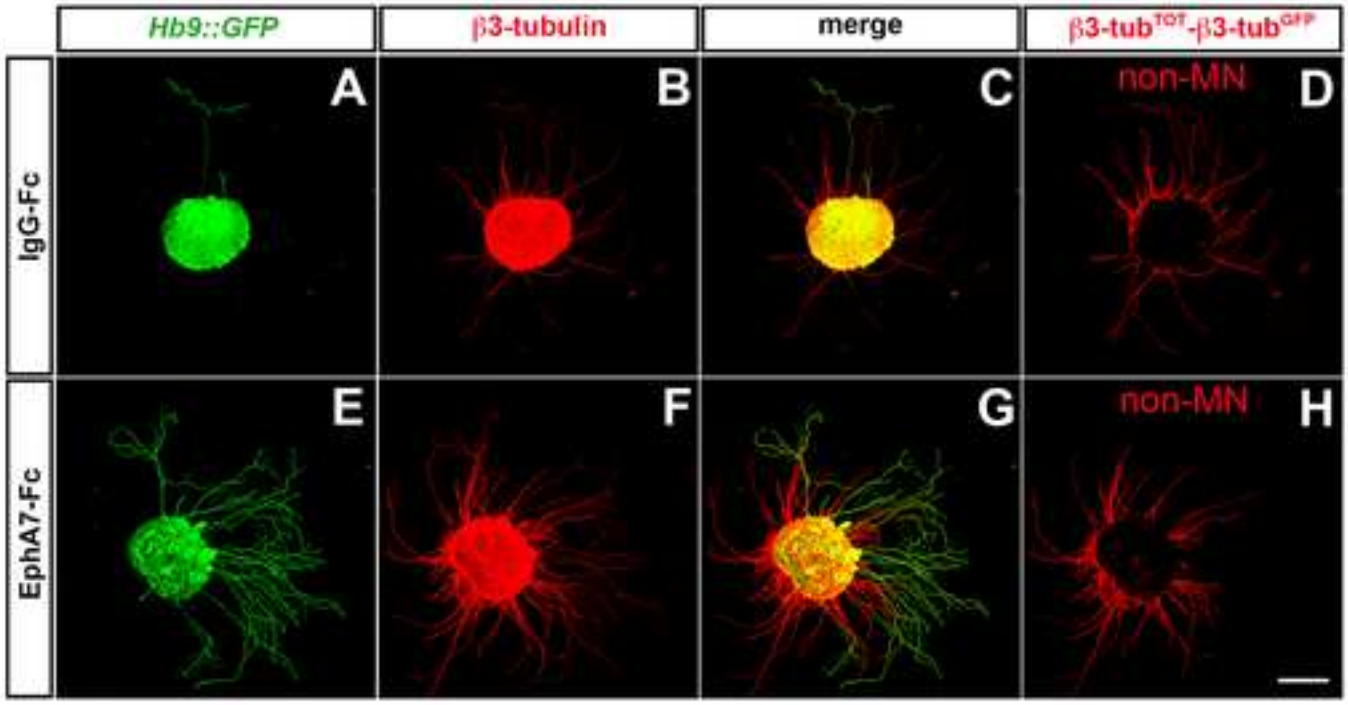

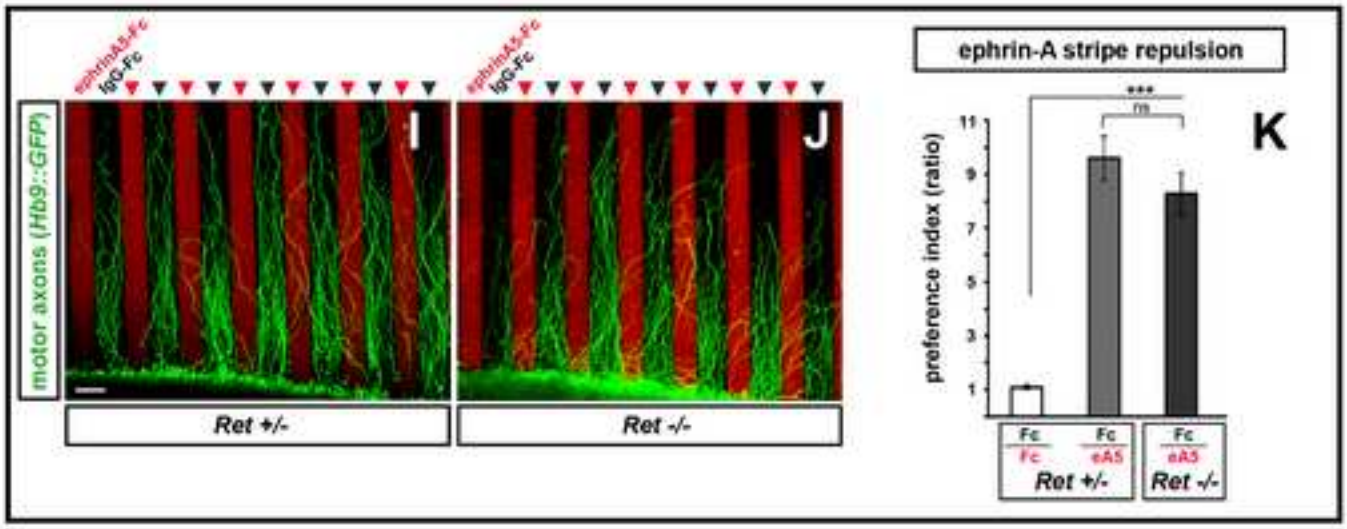

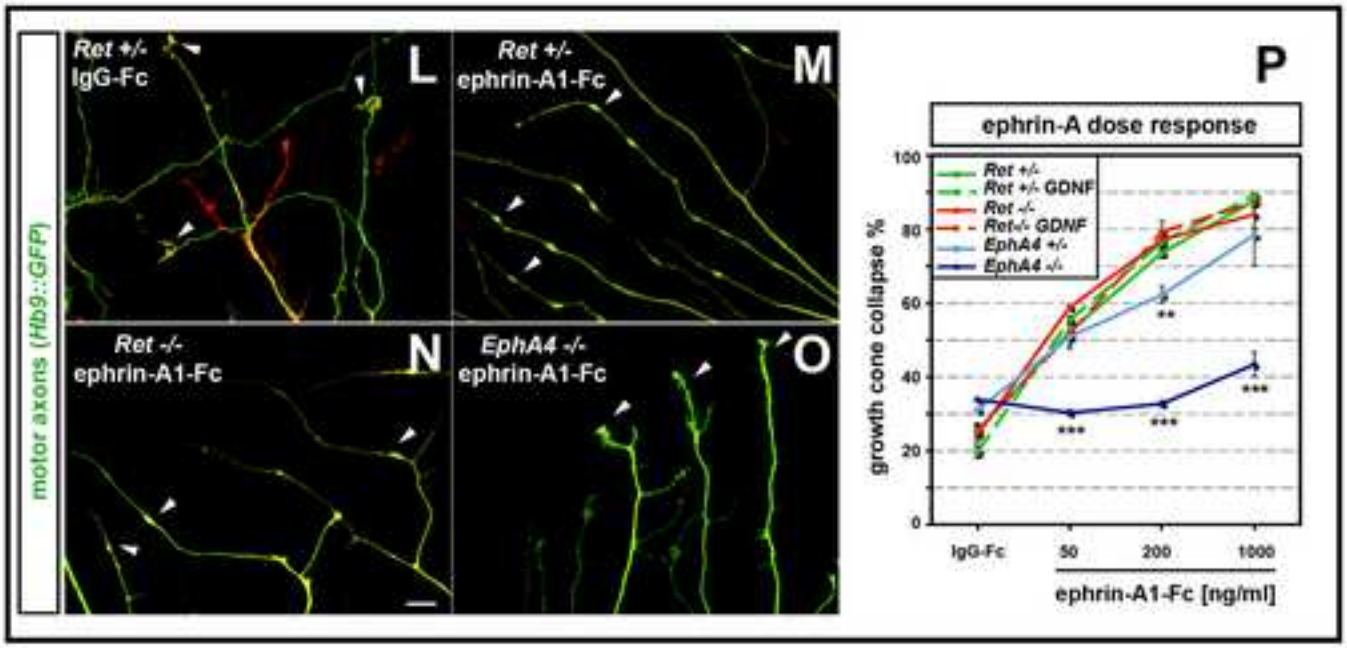

Supplemental Figure 5

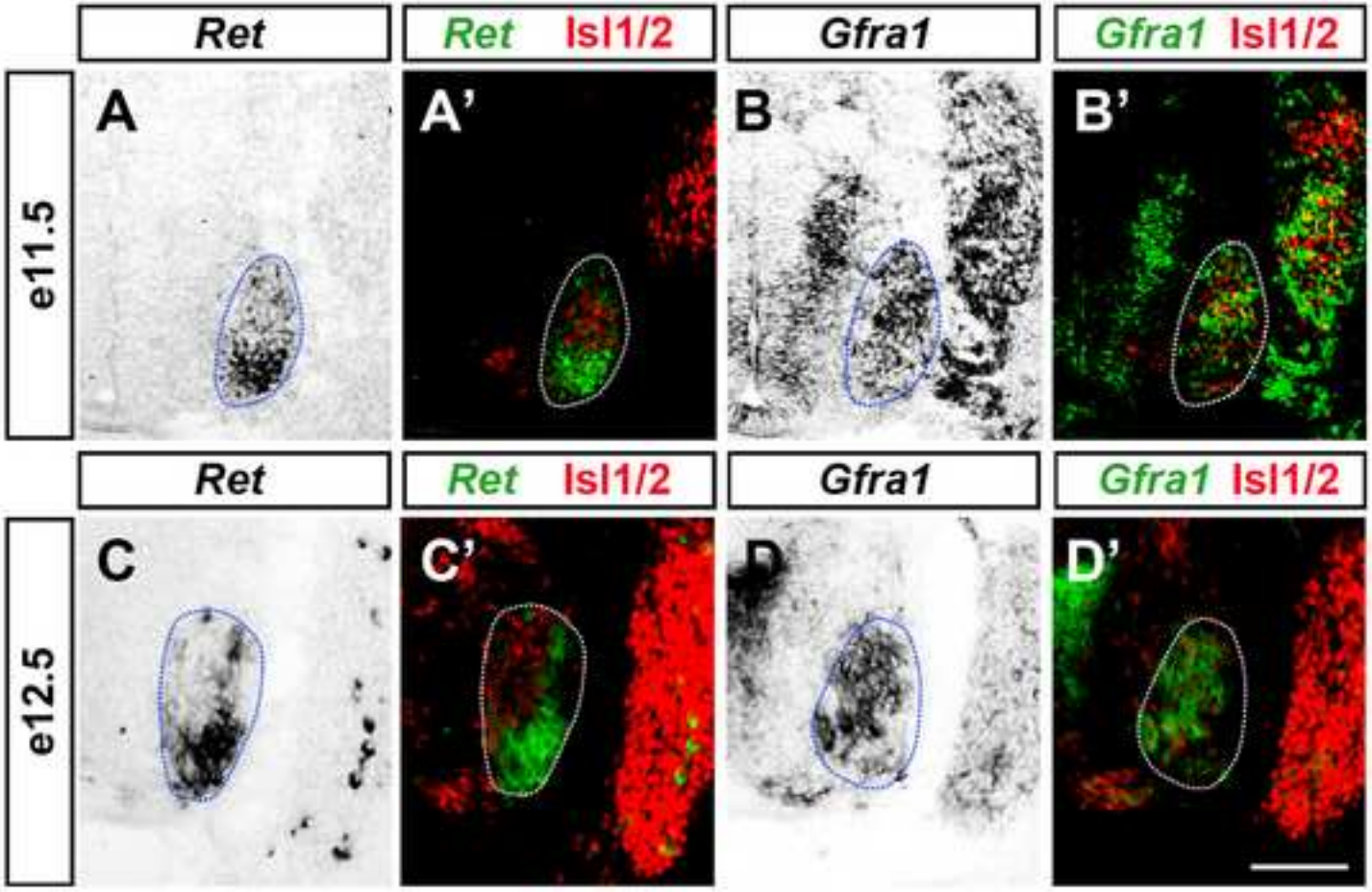

Supplemental Figure 6